JOURNAL OF CATALYSIS **174,** 88–97 (1998)
ARTICLE NO. CA971961

Adsorption Sites and Diffusion Mechanism of Alkylbenzenes in Large Pore Zeolite Catalysts as Predicted by Molecular Modeling Techniques

Ramesh Ch. Deka and Rajappan Vetrivel

Catalysis Division, National Chemical Laboratory, Pune 411 008, India

Received July 31, 1997; revised October 27, 1997; accepted October 27, 1997

In this work, we demonstrate the efficiency of force field energy minimization technique to study the adsorption and diffusion behavior of large molecules inside the micropores of zeolites. Molecular modeling studies for diffusion of alkylbenzene molecules, namely, ethylbenzene, *p*-diethylbenzene, isobutylbenzene, and *o*-, *m*-, and *p*-isobutylethylbenzene in various zeolites, such as faujasite, zeolite L, mazzite, and mordenite, indicate that mordenite is a good catalyst for selective synthesis of *p*-isobutylethylbenzene. The periodic variations of interaction energy between the molecules and zeolite framework in the calculated diffusion energy profiles are used to predict the energy barrier for diffusion. Force field energy minimization calculations for the cage to cage diffusion of the alkylbenzenes in faujasite show no significant diffusional energy barrier for any of the molecule. Zeolite L shows a very small selectivity toward *p*-isobutylethylbenzene which is due to a rapid change in minimum energy configuration as the molecules diffuse along the pore. In the case of mazzite, a high diffusional energy barrier is observed for *o*-isobutylethylbenzene compared to *m*- and *p*-isomers. Calculations of the diffusion energy profiles for the molecules in mordenite show that there is negligible energy barrier for the diffusion of *p*-isobutylethylbenzene, whereas an energy barrier of 17.95 kJ/mol exists for diffusion of *m*-isobutylethylbenzene and a significantly large energy barrier of 95.69 kJ/mol exists for *o*-isobutylethylbenzene. Thus, the efficiency of shape selective production of *p*-isobutylethylbenzene in these zeolites will be in the order faujasite ∼ zeolite L < mazzite < mordenite. The adsorption of the molecules in general are energetically favorable when the alkyl groups have maximum interaction with the surface of the zeolite pores. © 1998 Academic Press

INTRODUCTION

The structure of zeolite catalysts is characterized by the presence of regularly repeating intracrystalline cavities and pores, whose dimensions lie in the range 3–10 Å which is commensurable with molecular dimensions (1). A fascinating structure-related aspect of the zeolite catalysis is molecular shape selectivity (2–4). The subtle interplay of "configurational" diffusion and intrinsic kinetics of reactions in the intracrystalline pore system enable zeolite catalysts to differentiate between molecules or transition states involved in a reaction on the basis of their size and shape and thus direct the reaction along specific paths. The diffusion of molecules in zeolite pores plays the major role in this shape-selective process. The understanding of its mechanism can greatly facilitate the design of zeolite catalysts. The diffusional behavior of molecules in natural and synthetic zeolites is studied by several analytical (5–15) and computational (13–18) techniques. In the applications of zeolite catalysts, a clear picture of the nature and location of adsorbed molecules is of fundamental importance to understand the mechanism of the catalytic processes. The energetics of adsorption as a function of pore diameter has also been investigated experimentally (19). However, a systematic study of sorption in zeolites has not been performed and the experimental observations reported in the literature are sometimes contradictory.

Computer simulations, using molecular dynamics or Monte Carlo techniques, are an attractive alternative to experiments because these methods can, in principle, provide information for the conditions under which experiments are not feasible. Previous simulations, based on molecular dynamics calculations (20–22), Monte Carlo calculations (23), or hybrid Monte Carlo and energy minimization procedure (24), tended to concentrate on small guest molecules and until now these techniques are not used to study large molecules of catalytic relevance due to highly demanding computations.

Force field energy minimization technique is an efficient method for studying the location and conformation of large guest molecules within the micropores of zeolites. We demonstrate here that this approach can be extended to study diffusional behavior of alkylbenzenes in zeolites. We use this technique to study the adsorption and location of ethylbenzene (EB), *p*-diethylbenzene (*p*-DEB), isobutylbenzene (IBB), and *o*-, *m*-, and *p*-isomers of isobutylethylbenzene (IBEB) in large pore fully siliceous form of zeolites. The main objective of this work is to

0021-9517/98 $25.00

TABLE 1

Crystal Characteristics and the Dimensions of the Simulation Boxes for Different Zeolites

Zeolite	Symmetry	Unit cell composition	a (Å)	b (Å)	c (Å)	Average pore diameter (Å)	Number of unit cells
Faujasite	Cubic	$[SiO_2]_{192}$	25.028	25.028	25.028	7.4	2 × 2 × 2
Zeolite L	Hexagonal	$[SiO_2]_{36}$	18.465	18.465	7.476	7.1	2 × 2 × 8
Mazzite	Hexagonal	$[SiO_2]_{36}$	18.392	18.392	7.646	7.4	2 × 2 × 8
Mordenite	Orthorhombic	$[SiO_2]_{48}$	18.094	20.516	7.524	6.5 × 7.0	1.7 × 1.5 × 8

find out a suitable zeolite catalyst for selective synthesis of *p*-IBEB which is the key intermediate in the production of α-(4-isobutylphenyl) propionic acid, a popular analgesic drug called ibuprofen (25). The conventional synthesis route for the production of *p*-IBEB involves the alkylation of isobutylbenzene with ethene over Lewis acid catalysts (26) in which the selectivity toward *p*-IBEB is typically 17.6%. Recently, the possibility of using zeolite catalysts for the production of *p*-IBEB by disproportionation of isobutylbenzene and a polyalkylbenzene over HY zeolite (27) has been shown to lead to better selectivity (46.3%). Although HY zeolite is better than conventional catalyst, selection of this specific zeolite is a random choice rather than a logical selection and no experimental results are available for any other zeolites. Hence, we want to analyze the efficacy of different zeolites. We have chosen large pore zeolites with 1-d pores, where only single file diffusion is possible, zeolites with 2-d pores, where different molecular reorientation is possible at channel intersections, and zeolites with 3-d pores where cage to cage translations are possible, with total dynamic freedom inside the cages. The influence of change in pore architecture on adsorption and diffusion behavior of the molecules is studied in detail. Here, we describe the application of a combination of molecular modeling techniques such as molecular graphics, conformational analysis, and force field energy minimization claculations to search the most viable zeolite catalyst for the selective synthesis of *p*-IBEB. Favorable and unfavorable locations of adsorption sites for the molecules are also determined in this study.

METHODS

The minimum energy configurations of all the molecules are derived from force field energy minimization procedures using CVFF (consistent valence force field) expression (28). A conformational search analysis is carried out to determine the minimum energy configurations of each molecule as well as their flexibility. The dimensions of the molecules in three-dimensional space are measured according to the procedure detailed elsewhere (29). The molecular graphics analysis and the force field energy minimization calculations are carried out with the Insight II and Discover software packages supplied by Biosym Technologies Inc. (U.S.A.). All the calculations were carried out in a SiliconGraphics Indigo2 workstation. The diffusion energy profiles are calculated for the diffusion of EB, *p*-DEB, IBB, and *o*-, *m*-, and *p*-IBEB in large pore zeolites, namely, faujasite, zeolite L, mazzite, and mordenite. The crystal characteristics and the dimensions of the simulation boxes for these zeolites are given in Table 1. The zeolite structures are taken from the crystal structure reported for faujasite (30), zeolite L (31), mazzite (32), and mordenite (33).

The interaction energy of each of the molecule with the zeolite framework is calculated using the expression that contains the terms corresponding to deformation of bond lengths, bond angles, torsion angles, etc. (34). During the calculation of the interaction energy, the atoms in the zeolite lattice are assumed to be fixed at their crystallographically determined geometries. The sorbate molecule is forced to diffuse stepwise, in steps of 0.2 Å inside the 12-m channel between two points, which define the diffusion path. These two points are located at the mid-points of the pore apertures of the 12-m channel in zeolite L, mazzite, and mordenite. In the case of faujasite, three points are defined at the centers of three consecutive supercages and force field calculations are performed. After each step, a strong harmonic potential constrains the molecule to lie at a fixed distance from these points, while its orientation and conformation corresponding to minimum energy are chosen. Thus the interaction energy is minimized at each step with respect to the internal degrees of freedom as well as the nonbonding interactions with the zeolite framework. The nonbonding interactions of the molecules with the zeolite framework are calculated by determining the long-range forces by classical electrostatic interactions and short-range interactions in terms of Lennard–Jones potentials (28). The potential parameters used in the calculation are given in Table 2. Different starting orientation of the molecules and different directions of diffusion of molecules were considered in these calculations. In case of zeolite L, where several configurations are possible inside the "barrel-shaped" cage, the Monte Carlo technique was adopted to choose the most stable configuration.

TABLE 2

Parameters Used in Force Field Energy Minimization Calculations

Bond length parameters: $E = k_1\ (r - r_0)^2$

Atoms[a]		r_0 (Å)	k_1 (kcal mol^{-1} Å^{-2})
c	h	1.1050	340.6175
cp	h	1.0800	363.4164
cp	cp	1.3400	480.0000
cp	c	1.5100	283.0924

Bond angle parameters: $E = k_2\ (\theta - \theta_0)^2$

Atoms			θ_0	k_2 (kcal mol^{-1} degree^{-2})
h	c	h	109.4000	39.5000
h	c	c	110.0000	44.4000
cp	cp	h	120.0000	37.0000
cp	cp	cp	120.0000	90.0000
h	c	cp	110.0000	44.4000
c	cp	cp	120.0000	44.2000
cp	c	cp	110.5000	46.6000

Torsion parameter: $k_\phi\ (1 + \cos(n\phi - \phi_0))$

Atoms				k_ϕ (kcal mol^{-1})	n	ϕ_0
*	cp	cp	*	12.0000	2	180.000

Out-of-plane parameter: $E = k_\chi\ (1 + \cos(n\chi - \chi_0))$

Atoms				k_χ (kcal mol^{-1})	n	χ_0
cp	cp	cp	*	0.3700	2	180.0000

Nonbonded parameters:
$E = A_{ij}/r^{12} - B_{ij}/r^6$; $A_{ij} = (A_i A_j)^{1/2}$; $B_{ij} = (B_i B_j)^{1/2}$

Atoms	A (kcal mol^{-1} Å^{12})	B (kcal mol^{-1} Å^6)
h	7108.4660	32.87076
c	1790340.7240	528.48190
o	272894.7846	498.87880
cp	2968753.3590	1325.70810
si	3149175.0000	710.00000

[a] Atom types: h, hydrogen; c, aliphatic carbon; cp, aromatic carbon; o, zeolite oxygen; si, zeolite silicon.

* Any atom of the periodic table.

RESULTS AND DISCUSSION

Shape selectivity in catalytic reactions is governed by several factors such as kinetics of reaction (35) and the relative rates of diffusion of reactants, products, or reaction intermediates. The diffusivity and hence the shape selectivity is found to be dependent on the pore opening, the nature and number of acid sites, morphology, and the rate of coke formation (36–38). The possible reactant and product molecules are generated as molecular models and their minimum energy configurations are determined. We studied the diffusion energy profile of the reactant molecules such as EB, *p*-DEB, and IBB. There is rarely a constraint for the diffusivity of these molecules. In most cases, their diffusivities are of same order as that of *p*-IBEB or even higher and the reasons are discussed in the later section. We also studied in detail the diffusion energy profile of the product molecules.

The size and shape of the molecules are crucial parameters that decide their diffusivities. The molecular size of a guest molecule is usually characterized by a critical diameter, d_c, (39), a Lennard–Jones length constant, s_m (40), or a minimum kinetic diameter of the molecule, d_m (41). The molecular sizes defined by above methods pose problems, such as either they are too difficult to estimate or the estimated values are not reliable. We use more realistic values to describe the size and shape of the molecules, using conformational analysis. Conformational analysis is performed by allowing cooperative motion of the alkyl groups and the strain energy values for different conformers of the molecules are determined. For the energetically favorable conformation, the three largest dimensions (a × b × c) in mutually perpendicular directions of the molecules are given in Table 3. When correlating the dimensions of the molecules with the pore diameter of zeolites for molecular fitting purposes, it is customary to neglect the largest dimension (a) of the molecules (29). The molecules prefer to enter the cages through their smallest dimensions on the basis of interaction energy criteria. Hence, only the other two dimensions (b and c) of the molecules must be compared with the size of the pore openings. Comparing the dimensions (b and c) of the molecules in Table 3, it is observed that "small" (with 8-member rings) and "medium" (with 10-member rings) pore zeolites are too small to accommodate isomers of IBEB, while "large" pore zeolites are suitable for the diffusion of IBEB isomers.

When we consider the interactions between zeolites and sorbed molecules, the location and conformation of guest molecules within the micropores can have a profound effect on the subsequent chemistry of these systems. Molecular level information on the location and conformation of sorbed molecules is not always readily accessible by experimental means, and recent advances in theoretical methods have made interaction energy calculations combined with molecular graphics an ideal candidate to address these

TABLE 3

Dimensions of Different Organic Molecules as Derived form the Force Field Calculations

Molecules	Dimensions/Å		
	a	b	c
EB	6.32	4.97	2.74
p-DEB	8.47	5.28	4.23
IBB	7.93	5.07	3.88
m-IBEB	8.45	5.95	5.55
o-IBEB	7.50	6.85	4.61
p-IBEB	10.47	5.22	4.46

problems. A similar approach has been recently applied and proven successful to study the selectivity in the formation of different isomers of alkylnaphthalene (42) and the selectivity in the conversion of *n*-butene to isobutene in relation to several other products (43) inside zeolites. The diffusion energy profiles for different molecules give a good indication of the relative rates of diffusion through the pore of the zeolite. The diffusion energy profile is the graph showing the variation of interaction energy between the molecules and the zeolite framework as the molecule diffuses within the channel of the zeolite. These profiles are useful to identify the most favorable and unfavorable adsorption sites for the molecules inside the zeolite channels and the intraparticle diffusion is not covered in this procedure. The results of this study are useful for comparing the self-diffusion studies of molecules, particularly in relation to local diffusion behavior of molecules in zeolites for the membrane applications (44). The difference between the most favorable site (minimum energy) and the most unfavorable site (maximum energy) in the diffusion energy profile provides qualitative estimate of the diffusional energy barrier. For example, when energy barriers for all the three isomers of IBEB are comparable, their diffusion rates should be approximately the same.

We report here the diffusion characteristics of the alkylbenzenes in 12-m channels of a variety of different siliceous zeolites. The influence of molecular dimensions of alkylbenzenes in diffusing through the 12-m channel of mordenite has been the subject of our previous theoretical studies (45). In the present work, our emphasis is the influence of the pore architecture of different zeolites such as faujasite, zeolite L, mazzite, and mordenite.

(a) Faujasite. Faujasite is a 3-dimensional zeolite with cubic symmetry, having 12-m ring openings of 7.4 Å in diameter that provide access to a supercage of diameter 12.4 Å. In our calculations, the diffusion paths for the alkylbenzenes in faujasite are defined by three points (A, B, and C) at the centers of three consecutive supercages. The molecular graphics picture in Figure 1 shows the three supercages and diffusion path of the molecules from A to C, via B. Figure 1 includes the diffusion energy profile for

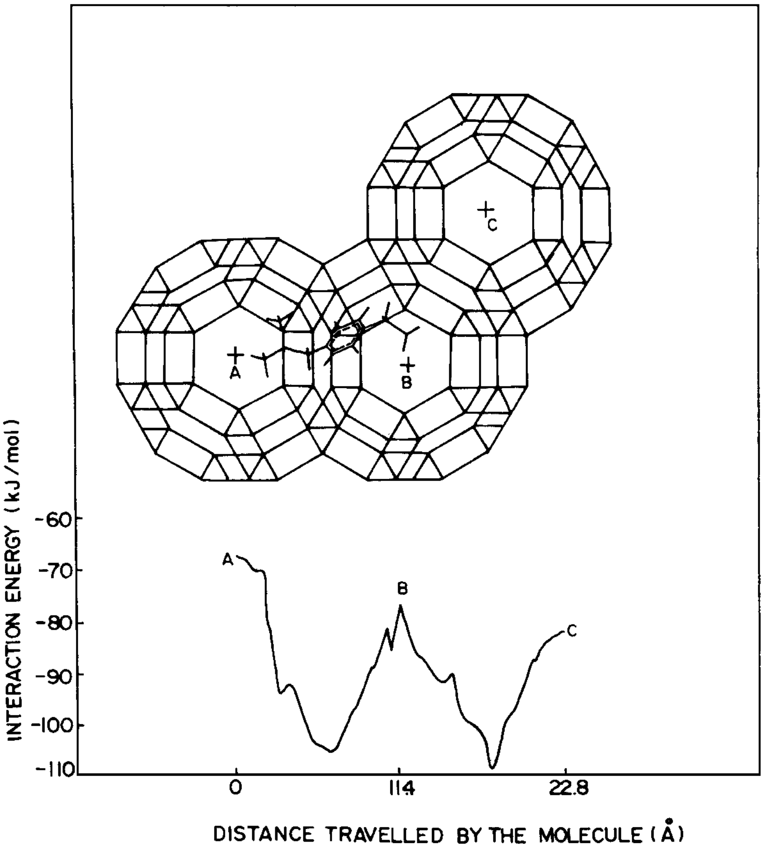

FIG. 1. Variation of interaction energy of *p*-IBEB with faujasite lattice during cage-to-cage diffusion through 12-m windows. The molecular graphics picture depicts the three supercages in different planes of the faujasite lattice. A typical minimum energy configuration of *p*-IBEB during the diffusion calculation is shown. A, B, and C in the molecular graphics picture show the center points of the three supercages. In the graph, A, B, and C show the interaction energy values at the center points of three supercages.

TABLE 4

Diffusional Energy Barriers in kJ/mol for Different Molecules in Large Pore Zeolites

	Zeolites			
Alkylbenzenes	Faujasite	Zeolite L	Mazzite	Mordenite
EB	26.92	38.69	14.09	6.74
p-DEB	35.36	38.09	7.65	7.82
IBB	31.65	35.87	11.21	10.13
m-IBEB	28.38	43.69	9.78	17.95
o-IBEB	32.74	40.87	50.78	95.69
p-IBEB	31.65	28.43	10.69	6.44

p-IBEB in faujasite. The minimum energy configuration of *p*-IBEB in faujasite is also shown in Fig. 1. It is clear from Fig. 1 that when the molecule moves from one supercage to another the molecule energetically prefers to be near the wall rather than at the center of the supercage. Its interaction energy decreases and becomes minimum when the benzene ring of *p*-IBEB is at the center of the 12-member ring. As the molecule diffuses towards the center of the second supercage from 12-m ring its interaction energy increases and again becomes maximum at the center of the second supercage. Due to this high energy conformer, a diffusional energy barrier exists for cage to cage diffusion of the molecule in faujasite. Similar diffusional profiles are calculated for EB, *p*-DEB, IBB, *m*-IBEB, and *o*-IBEB and the overall behavior of the molecules are found to be the same. The diffusional energy barriers of all the alkylbenzenes are given in Table 4. It is seen from Table 4 that the energy barriers for diffusions of all the molecules are almost in the same order. We may conclude from this analysis that the pore system of faujasite places little constraint on the diffusion of different molecules. Hence, faujasite may not be an efficient shape selective zeolite catalyst for selective synthesis of *p*-IBEB.

(b) Zeolite L. Zeolite L belongs to the hexagonal crystal class. The pore in zeolite L is circular with a pore diameter of 7.1 Å. It has a structure consisting of channels along the c direction. The channels are built up of “barrel-shaped” cages that are interconnected via 12-member pores. The 12-m rings are separated by 7.5 Å along the c direction. The diameter of the barrel is largest (12.6 Å) at the midway between the two consecutive 12-m rings. In the regions of the pore, midway between the two 12-m rings, there is sufficient room for the sorbate to adopt several tilted configurations with the ethyl and isobutyl groups projecting in different orientations with respect to the 12-m channel, as shown in Fig. 2. The diffusion path for the molecules is defined by a pair of points (A and B) on the channel axis at opposite ends of the section of the channel under investigation, as shown in Fig. 3, and the diffusion calculations are carried out in the same way as in faujasite. However, the calculation of energy profiles for the molecules in zeolite L are far from straightforward. A series of sharp peaks with high intensity is observed at regular intervals for *m*- and *p*-IBEB in zeolite L. These sharp peaks in zeolite L are due to the barrel shaped cage between two 12-m rings. The tilted (minimum energy) configuration of *p*-IBEB in zeolite L is shown in Fig. 2A. This configuration favors the interaction between the sorbate and the zeolite framework and thus is a preferred configuration in this region of the pore. The view of the minimum energy configuration of *p*-IBEB along the channel axis is shown in Fig. 2B. However, during the diffusion through the channel the sorbate must adopt a configuration in which the benzene ring is parallel to the pore axis. The change in the orientation of the molecule is necessitated by the specific pore architecture of zeolite L. The sorbate in the tilted configuration (Fig. 2A) must cross over an energy barrier to find the new preferred configuration. As the molecule diffuses in the direction of diffusion path, the interaction energy value rises sharply because the ethyl and isobutyl groups are forced to adopt a strained configuration (Fig. 2C) with respect to the benzene ring before the molecule can take a parallel orientation. After advancing a short distance, however, the sorbate is forced to the normal nontilted configuration (Fig. 2D) and the interaction energy immediately drops to a lower value. During the force field calculations, such spurious peaks are known to occur (42). This artifact was avoided by carrying out Monte Carlo calculations for the random search of the equilibrium configurations. Thus the equilibrium configuration is obtained by a more efficient procedure. This configuration is further considered for the force field calculation of the interaction energy.

The energy profiles for *p*-IBEB in zeolite L calculated with combined Monte Carlo and force field energy minimization techniques are shown in Fig. 3 and the diffusional energy barriers for all the molecules are given in Table 4. From Table 4, it is seen that as in the case of faujasite there is no significant difference in the energy barrier for diffusion of the molecules in zeolite L. These calculations bring out the significance of the pore architecture. Zeolite L, with 2-dimensional pores is also not efficient shape selective catalyst for the production of *p*-IBEB as in the case with 3-dimensional faujasite.

(c) Mazzite. Zeolite mazzite is another hexagonal but one dimensional zeolite with pore diameter of 7.4 Å. Two types of smaller channels are present: the first consists of stacked gmelinite cages surrounded by six-member rings; the second is between two cross-linked rows of cages and is surrounded by eight-member rings. The calculated diffusional energy barriers for the molecules in mazzite are given in Table 4. It can be seen from Table 4 that the diffusional energy barriers for EB, IBB, *p*-DEB, *m*-IBEB, and *p*-IBEB are in the same order, whereas there is a significantly high energy barrier for *o*-IBEB.

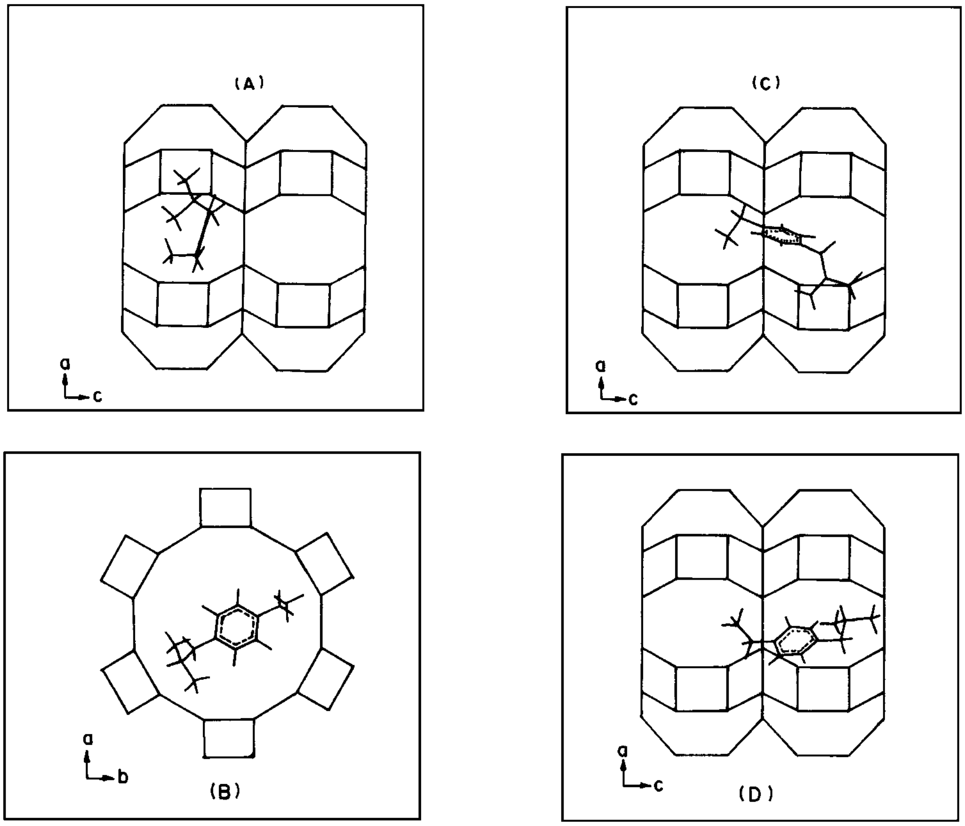

FIG. 2. The molecular graphics picture showing the *p*-IBEB at various locations along the 12-m channel of zeolite L. The minimum energy configuration of *p*-IBEB is shown in (A), when it is at the center of the barrel-shaped cage. The same minimum energy configuration as viewed from a perpendicular direction that is along the axis of the 12-m channel is shown in (B). The configuration of *p*-IBEB (C) when it is crossing the 12-m ring connecting the barrels and the configuration (D) while diffusing toward the center of the barrel are also shown. The configurations C and D have higher energy values.

The diffusion energy profile for *p*-IBEB in mazzite is plotted graphically in Fig. 4. In the same figure the minimum and maximum energy configurations are also shown. The molecule passes through energy maxima and minima when it diffuses through the channel. There are alternative 8-m pocket in the channel of mazzite. The molecule adopts a minimum energy configuration when its phenyl ring is at the center of 8-m ring and the alkyl groups point toward other two 8-m rings. In other words, the maximum energy corresponds to the configuration in which phenyl ring as well as both the alkyl groups are in between the 8-m rings. Since there exists an energy barrier for diffusion of *o*-IBEB in mazzite, the diffusivity of other two isomers will be relatively faster than *o*-IBEB and mazzite will be more selective catalyst compared to faujasite and zeolite L.

(d) Mordenite. Zeolite mordenite belongs to orthorhombic symmetry and has a pore structure that is effectively unidimensional. An elliptical 12-m channel (6.5×7.0 Å) runs parallel to [001] and has small side pockets (2.6×5.7 Å) parallel to the [010] direction which connect to the next 12-m channel. The calculated diffusional energy barriers of the molecules in mordenite are given in Table 4. It can be seen that the diffusional energy barriers for the isomers of IBEB are significantly different even though there are only small variation in the dimensions of the molecules. These results indicate the significance of the pore dimensions also, since the mordenite has small pore dimensions compared to other zeolites considered in this study. The diffusional energy barriers for *p*-IBEB and diffusion track for three carbon atoms (one aromatic carbon, two alkylcarbons) are shown in Fig. 5. The molecule passes through energy maxima and minima while diffusing through a unit cell; the variation of interaction energy values symmetrically repeats in the second and third unit cells also as shown in Fig. 5. It is evident that the diffusion of the reactant molecules, namely EB, *p*-DEB, and IBB have energy barriers of 6.74, 7.82, and 10.13 kJ mol^{-1}, respectively. The energy barrier for the diffusion of *p*-IBEB is also of the same order (6.44 kJ mol^{-1}). However, there exists an energy barrier of 17.95 kJ mol^{-1} for *m*-IBEB and a significantly large energy barrier of 95.69 kJ mol^{-1} for *o*-IBEB.

From the diffusion track of the different carbon atoms it is seen that as the alkyl groups move toward the zeolite

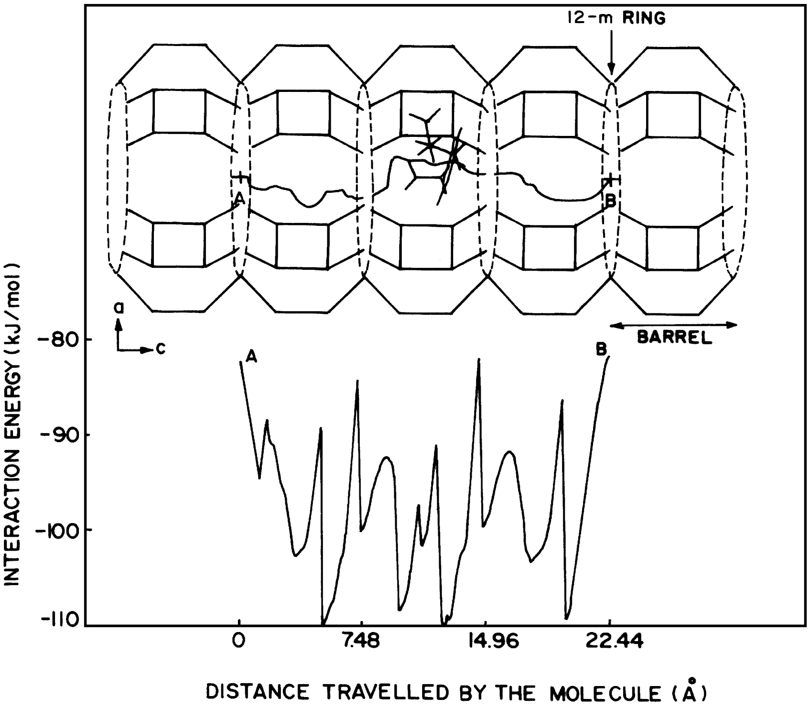

FIG. 3. Variation of interaction energy of *p*-IBEB with zeolite L lattice during its diffusion along the *c*-axis through the barrel-shaped cages. The molecular graphics picture shows the diffusion path of the molecule alongwith a typical minimum energy configuration of *p*-IBEB during the diffusion.

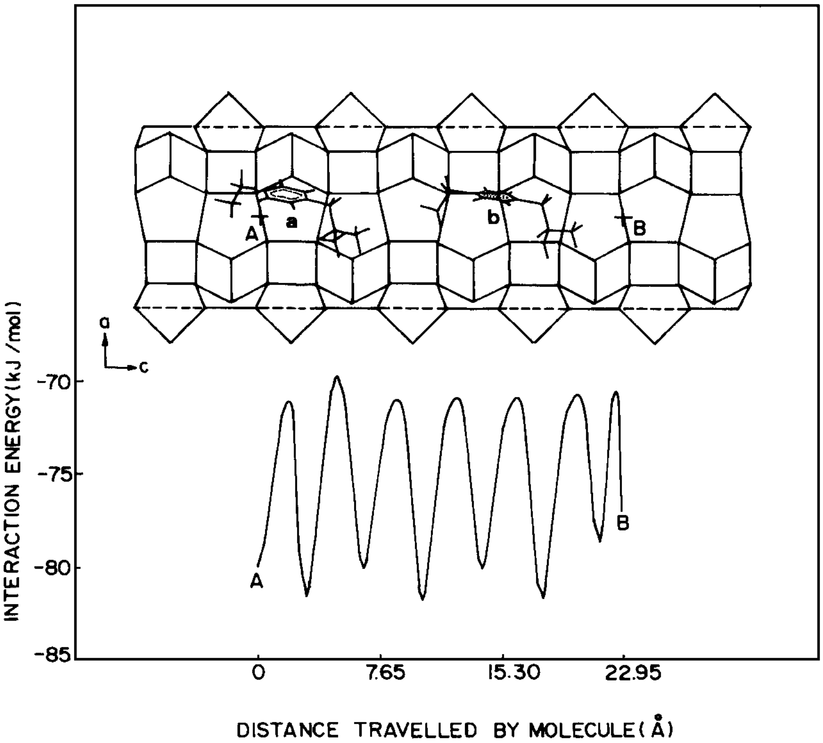

FIG. 4. Variation of interaction energy of *p*-IBEB with mazzite framework as the molecule diffuses through 12-m channel. A typical minimum (a) and a maximum (b) energy configurations of the molecule are shown.

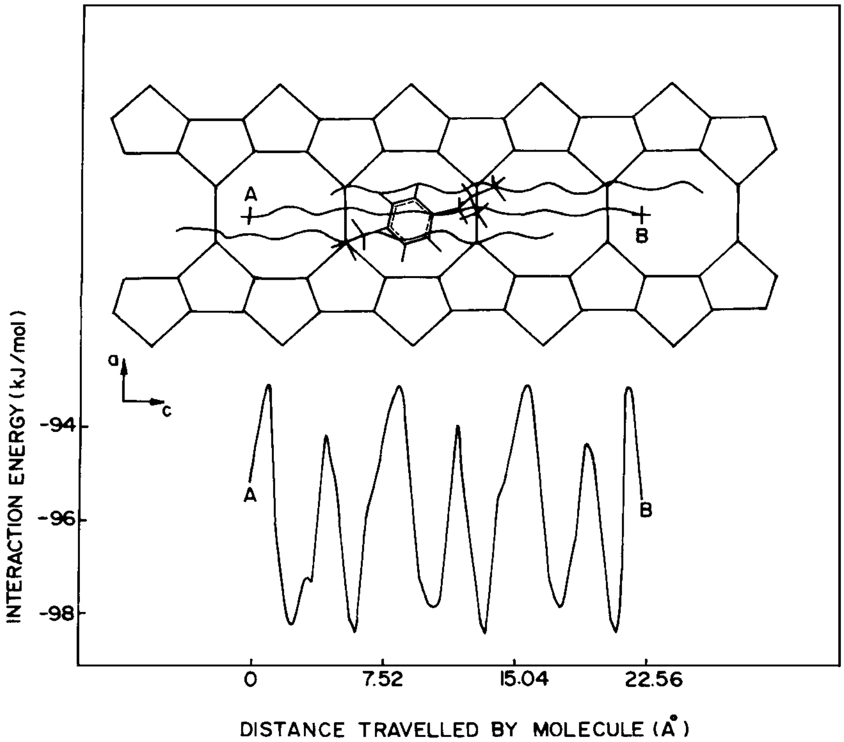

FIG. 5. Variation of interaction energy of *p*-IBEB with mordenite framework as the molecule diffuses through the 12-m channel. The diffusion tracks for the motion of three carbon atoms are shown. The diffusion tracks of aromatic carbon atom to which the isobutyl group is bonded (a), the primary carbon in the isobutyl group (b), and the primary carbon in the ethyl group (c) are indicated to bring out their freedom of motion during the diffusion.

framework its interaction energy decreases and becomes minimum. At maximum interaction energy, the molecule is parallel to the channel and the alkyl groups lie at the farthest distance from the zeolite framework. The same trend is found for diffusion of other molecules in mordenite.

These results also provide the information on the nature of sites inside mordenite where the molecules have favorable and unfavorable interactions. Figure 5 shows the position of *p*-IBEB in mordenite at its minimum energy configuration. It is seen from the figure that the molecule passes through two maxima and two minima, when it crosses each 8-m ring. The 8-m ring can be divided into four quarters. It is observed that when the phenyl ring of the molecule is at the beginning (0), center (0.5), or end (1) of the 8-m ring, the interaction of the molecule with the framework is most favorable while the unfavorable interaction corresponds to a configuration in which the phenyl ring is 0.25 or 0.75 through the 8-m ring. It is also observed that the favorable orientations of the molecule inside the 12-m ring are those in which the plane of the phenyl ring is parallel to the 8-m channel opening.

(e) Influence of pore architecture. From these studies we have seen that diffusion of molecules in zeolites depends on two important parameters, namely: (i) on the size of the molecules and (ii) on the pore diameter of the zeolites. The size and shape of the molecules are more flexible. In fact, the flexibility of the isomers of IBEB studied by conformational analysis indicate that their flexibility is in the order $p > m > o$. When the zeolite pore diameters match the dimensions of the molecules, the considerable increase in the diffusional energy barriers of *o*-IBEB and *m*-IBEB, compared to *p*-IBEB, can be related to their flexibility. From the results presented here, the influence of pore architecture and pore dimensions could be discussed in detail. The figures presented here are typically for *p*-IBEB; however, the *o*- and *m*-IBEB also follow almost the same trend but with varying diffusion energy barriers. As mentioned above, all the diffusion energy barrier values extracted from these studies are summarized in Table 4. In general, it can be observed that “channel-like” architecture as in mazzite and mordenite are good for the selectivity of *p*-IBEB than “cage-like” architectures as in the case of faujasite and zeolite L. Cages which are large enough to accommodate all the molecules are leading to uniform diffusion behavior for all the molecules with different sizes.

When the molecules diffuse through the channels of zeolites, they pass through surface and windows. From the analysis of the orientation and location of molecules in the minimum and maximum energy conformations, we observe that the alkyl groups in the molecules have favorable interaction with the surface in the zeolite framework, while the phenyl ring has an unfavorable interaction. As observed in the case of faujasite and zeolite L, the molecules prefer to change their orientation in which the alkyl groups can have more interaction with the surface. In mazzite also the adsorption sites, where alkyl groups are facing the 8-m windows in the zeolite framework, are unfavorable. In mordenite, for all the isomers of IBEB, the alkyl groups have an end-to-end vector along the channel axis with phenyl plane facing the 8-m side pockets, during the diffusion. The "window effect" discovered by Gorring (46) describes the nonlinear relation between the diffusion coefficient and size of the molecule. Our results provide qualitative explanation based on the interaction of molecule with the surface and windows inside channels. However, it is necessary to calculate the electronic interactions of the alkyl and phenyl groups with the side pockets and pore walls of the zeolite to understand the window effect quantitatively.

In addition to the size as well as shape of the reactant molecules and the dimensions as well as architecture of the pores, there are factors such as Si/Al ratios, the number and nature of exchanged cations, temperature which influence the vibration of the framework, and the nature of transition state also influence the shape selectivity in a minor way. ZSM-5 is known to be the best catalyst for the selective production of *p*-xylene than any other zeolite, independent of the Si/Al ratios and the exchanged cations (47), which emphasize the importance of pore architecture. The transition state for the *p*-IBEB would be more "linear." It is reasonable to assume that the transition states for the formation of *m*- and *o*-isomers can have somewhat "bent" configuration, like *m*- and *o*-isomers themselves, resulting in higher activation energy values for production of *m*- and *o*-IBEB. Although the medium pore zeolites seem suitable for the diffusion of reactant and product molecules, the formation of transition state for any of the isomer will be difficult.

CONCLUSIONS

From the results presented here and in light of the above discussions, the salient features of the diffusion of IBEB can be summarized as given below.

(i) The diffusional characteristics of these molecules in the zeolite lattice depend on the molecular dimensions and the pore architecture of the zeolite.

(ii) The molecule–lattice interactions control the diffusion mechanism of molecules through the channel of a zeolite. The molecules prefer the configurations, where there is maximum interaction between the surface of the zeolite and the alkyl groups of the molecules.

(iii) Force field energy minimization calculation of the diffusion energy profile is simple technique relative to experimental studies of diffusion and reliable technique for logical catalyst screening.

(iv) These calculations show that significant energy barriers exist for *m*- and *o*-IBEB in mordenite, *o*-IBEB in mazzite, and for none of them in faujasite and zeolite L. Hence the order of selectivity in shape selective production of *p*-IBEB in these zeolites will be mordenite $>$ mazzite $>$ zeolite L $\sim$ faujasite.

ACKNOWLEDGMENT

The authors thank CSIR, New Delhi, for the financial support in the form of Senior Research Fellowship to R.C.D.

REFERENCES

1. Riekert, L., *in* "Advances in Catalysis" (D. D. Eley, H. Pines, and P. B. Weisz, Eds.), Vol. 21, p. 281. Academic Press, New York, 1970.
2. Weisz, P. B., *in* "New Horizons in Catalysis" (T. Seiyama and K. Tanabe, Eds.), Vol. 7A, p. 3. Elsevier, Amsterdam, 1981.
3. Weisz, P. B., *Chemtech* **3**, 498 (1973).
4. Derouane, E. G., *in* "Catalysis by Zeolites" (B. Imelik, C. Naccache, Y. B. Taarit, J. C. Vedrine, G. Coudurier, and H. Praliaud, Eds.), Vol. 5, p. 5. Elsevier, Amsterdam, 1980.
5. Satterfield, C. N., and Katzer, J. R., *Adv. Chem. Ser.* **102**, 193 (1971).
6. Bülow, M., Struve, P., Finger, G., Redszus, C., Ewrhardt, K., Schirmer, W., and Kärger, J., *J. Chem. Soc., Faraday I* **76**, 597 (1980).
7. Haag, W. O., Lago, R. M., and Weisz, P. B., *Faraday Dis. Chem. Soc.* **72**, 317 (1981).
8. Eckman, R. R., and Vega, A. J., *J. Phys. Chem.* **90**, 4679 (1986).
9. Pfeifer, H., *Phys. Rep.* **26C**, 293 (1976).
10. Jobic, H., Renouprez, A., Bee, M., and Poinsignon, C., *J. Phys. Chem.* **90**, 1059 (1986).
11. Yasuda, Y., and Yamamoto, A., *J. Catal.* **93**, 176 (1985).
12. Caro, J., Bülow, M., Jobic, H., Kärger, J., and Zibrowius, B., *in* "Advances in Catalysis" (D. D. Eley, H. Pines, and P. B. Weisz, Eds.), Vol. **39**, p. 351. Academic Press, New York, 1983.
13. Ruthven, D. M., "Principles of Adsorption and Adsorption Processes." Wiley, New York, 1984.
14. Karger, J., and Ruthven, D. M., "Diffusion in Zeolites and other Microporous Solids." Wiley, New York, 1992.
15. Chmelka, B. F., Raftery, D., McCormick, A. V., de Menorval, L. C., Levine, R. D., and Pines, A. *Phys. Rev. Lett.* **66**, 580 (1991).
16. Kärger, J., Petzold, M., Pfeifer, H., Ernst, S., and Weitkamp, J., *J. Catal.* **136**, 283 (1992).
17. Xiao, J., and Wei, J., *Chem. Eng. Sci.* **47**, 1143 (1992).
18. Catlow, C. R. A. (Ed.), "Modelling of Structure and Reactivity in Zeolites." Academic Press, London, 1992.
19. Stach, H., Jänchen, J., Thamm, H., Stiebitz, E., and Vetter, R. A., *Adv. Sci. Technol.* **3**, 261 (1986).
20. Yashonath, S., and Santikary, P., *J. Phys. Chem.* **97**, 13778 (1993).
21. June, R. L., Bell, A. T., and Theodorou, D. N., *J. Phys. Chem.* **96**, 1051 (1992).
22. Dumont, D., and Bougeard, D., *Zeolites* **15**, 650 (1995).
23. Goodbody, S. J., Watanabe, K., MacGowan, D., Walton, J. P. R. B., and Quirke, N., *J. Chem. Soc., Faraday Trans.* **87**, 1951 (1991).
24. Freeman, C. M., Catlow, C. R. A., Thomas, J. M., and Brode, S., *Chem. Phys. Lett.* **186**, 137 (1991).
25. Rieu, J.-P., Boucherle, A., Cousse, H., and Mouzin, G., *Tetrahedron* **42**, 4095 (1986).
26. Shimizu, I, Matsumura, Y., Tokumoto, Y., and Uchida, K., European Patent Applications EP 373 362, June 20, 1990.

27. Tokumoto, Y., Shimizu, I., and Inoue, S., European Patent Application, EP 414 207, February 27, 1991.
28. Dauber-Osguthorpe, P., Roberts, V. A., Osguthorpe, D. J., Wolff, J., Genest, M., and Hagler, A. T., *Proteins: Struct. Funct. Genet.* **4**, 31 (1988).
29. Chatterjee, A., and Vetrivel, R., *J. Chem. Soc., Faraday Trans.* **91**, 4313 (1995).
30. Olson, D. H., *J. Phys. Chem.* **74**, 2758 (1970).
31. Newsam, J. M., *J. Phys. Chem.* **93**, 7689 (1989).
32. Galli, E., *Cryst. Struct. Commun.* **3**, 339 (1974).
33. Alberti, A., Davoli, P., and Vezzalini, G., *Z. Kristallogr.* **175**, 249 (1986).
34. Hagler, A. T., Lifson, S., and Dauber, P., *J. Am. Chem. Soc.* **101**, 5122 (1979).
35. Morin, S., Gnep, N. S., and Guisnet, M., *J. Catal.* **159**, 296 (1986).
36. Bhat, Y. S., Das, J., Rao, K. V., and Halgeri, A. B., *J. Catal.* **159**, 368 (1996).
37. Kim, J.-H., Ishida, A., Okajima, M., and Niwa, M., *J. Catal.* **161**, 387 (1996).
38. Chen, W.-H., Pradhan, A., Jong, S.-J., Lee, T.-Y., Wang, I., Tsai, T.-C., and Liu, S.-B., *J. Catal.* **163**, 436 (1996).
39. Ruthven, D. M., *Am. Chem. Soc. Symp. Ser.* **40**, 320 (1977).
40. Flanigen, E. M., Bennett, J. M., Grose, R. W., Cohen, J. P., Patton, R. L., and Kirchner, R. M., *Nature* **271**, 512 (1978).
41. Breck, D. W., "Zeolite Molecular Sieves." Wiley, New York, 1974.
42. Horsley, J. A., Fellmann, J. D., Derouane, E. G., and Freeman, C. M., *J. Catal.* **147**, 231 (1994).
43. Millini, R., and Rossini, S., *Stud. Surf. Sci. Catal.* **105**, 1389 (1996).
44. Bhave, R. R., "Inorganic Membranes: Synthesis, Characteristics and Applications." Van Nostrand–Reinhold, New York, 1991.
45. Deka, R. C., and Vetrivel, R., *Chem. Commun.* 2397 (1996).
46. Gorring, R. L., *J. Catal.* **31**, 13 (1973).
47. Chandwadkar, A. J., Abdulla, R. A., Hegde, S. G., and Nagy, J. B., *Zeolites* **13**, 470 (1993).